Lab on a Chip

PAPER

View Article Online
View Journal

Cite this: DOI: 10.1039/d2lc00508e

High-performance blood plasma separation based on a Janus membrane technique and RBC agglutination reaction†

Bing Xu, ‡*[ab] Juan Zhang,‡[a] Deng Pan,[c] Jincheng Ni,[d] Kun Yin,[e] Qilun Zhang,[f] Yinlong Ding,[g] Ang Li,[a] Dong Wu *[g] and Zuojun Shen *[a]

Separation of plasma which is full of various biomarkers is critical for clinical diagnosis. However, the point-of-care plasma separation often relies on microfluidic filtration membranes which are usually limited in purity, yield, hemolysis, extraction speed, hematocrit level, and protein recovery. Here, we have developed a high-performance plasma membrane separation technique based on a Janus membrane and red blood cell (RBC) agglutination reaction. The RBC agglutination reaction can form larger RBC aggregates to separate plasma from blood cells. Then, the Janus membrane, serving as a multipore microfilter to block large RBC aggregates, allows the plasma to flow from the hydrophobic side to its hydrophilic side spontaneously. As a result, the separation technique can extract highly-purified plasma (99.99%) from whole blood with an ultra-high plasma yield (~80%) in ~80 s. Additionally, the separation technique is independent of the hematocrit level and can avoid hemolysis.

Received 6th June 2022,
Accepted 11th October 2022

DOI: 10.1039/d2lc00508e

rsc.li/loc

1. Introduction

Plasma hosts many components including proteins, metabolites, and other substances which can be utilized as indicators of various diseases.[1] However, the presence of blood cells in blood constantly interferes with the detection procedures and affects the diagnosis results. Thus, plasma separation from blood cells is a critical step for blood-based clinical diagnostics.

Generally, ideal plasma separation methods for point-of-care testing (POCT) applications should satisfy the following metrics: rapid separation, high yield/purity, independence from the hematocrit level, prevention of hemolysis, and high protein recovery.[1] Conventional plasma separation is achieved through centrifugation which requires bulky, expensive and electricity-powered equipment.[2] As an alternative to centrifugation, many researchers have proposed active and passive microfluidic-based blood plasma separation technologies. The active separation approaches apply an external force to induce plasma extraction, including acoustic, electrical or magnetic fields.[3] However, these methods still require bulky equipment and complex fabrication processes. In comparison, the passive approaches, including microfluidic sedimentation,[4] microfiltration,[5–7] deterministic lateral displacement (DLD)[8,9] and inertial effects,[10,11] can realize plasma separation from blood cells by leveraging only physical forces within the flow. In particular, the microfiltration method (filtration membrane) is widely applied because it is simple and robust and it does not need complex devices or chip design.[5–8] For example, Hauser *et al.* employed a commercial hydrophilic multipore membrane to fabricate a passive blood plasma extraction device, where the extraction plasma yield was ~65% from human whole blood (hematocrit range of 35–55%) within 10 min.[5] Moreover, Mace group designed a passive plasma separator with two filters, where the first prefilter removed most of the white blood cells from the sample and the second hydrophilic plasma separation membrane excluded the remaining red

[a] *Department of Clinical Laboratory, The First Affiliated Hospital of USTC, Division of Life Sciences and Medicine, University of Science and Technology of China, Hefei, Anhui, 230001, China. E-mail: xb022@ustc.edu.cn, zuojunshen@ustc.edu.cn*
[b] *School of Mechanical Engineering, Suzhou University of Science and Technology, Suzhou, 215009, China*
[c] *College of Optoelectronics, Taiyuan University of Technology, Taiyuan 030024, China*
[d] *Department of Electrical and Computer Engineering, National University of Singapore, 117583 Singapore, Singapore*
[e] *School of Global Health, Chinese Center for Tropical Diseases Research, Shanghai Jiao Tong University School of Medicine, No. 227 Chongqing South Road, Shanghai 200025, China*
[f] *Laboratory for Diabetes, Department of Endocrinology, The First Affiliated Hospital of USTC, Division of Life Sciences and Medicine, University of Science and Technology of China, Hefei, China*
[g] *CAS Key Laboratory of Mechanical Behavior and Design of Materials, Department of Precision Machinery and Precision Instrumentation, University of Science and Technology of China, Hefei, 230026, China. E-mail: dongwu@ustc.edu.cn*

† Electronic supplementary information (ESI) available. See DOI: https://doi.org/10.1039/d2lc00508e

‡ Equal contribution.

blood cells to extract pure plasma.[12] The maximum plasma yield was ~53.8% (whole blood: 30% hematocrit) and the extraction time was within 10 min. Usually, in order to improve the plasma yield, the blood was introduced on the top of the hydrophilic plasma membrane. Although the hydrophilic plasma separation membrane[4,12,13] can provide a self-driving force to let the plasma continuously flow, the hydrophilic multipore membrane inevitably absorbs several plasma, resulting in the decrease of the plasma yield (Fig. 1a). In addition, to extract ultrapure plasma, nanopores are always constructed onto the filter membranes,[4,12] which sharply increases the plasma flow resistance and reduces the extraction speed (Fig. 1a). To reduce the plasma adhesion on the membrane and improve the residual plasma inside the membrane, a plasma separator with a superhydrophobic nanopore membrane[4] was reported by Liu *et al.* Whole blood was introduced on the bottom of the hydrophobic plasma membrane, which could reduce the membrane blockage by blood cells and increase the membrane separation capacity. As a result, the hydrophobic plasma separator can effectively

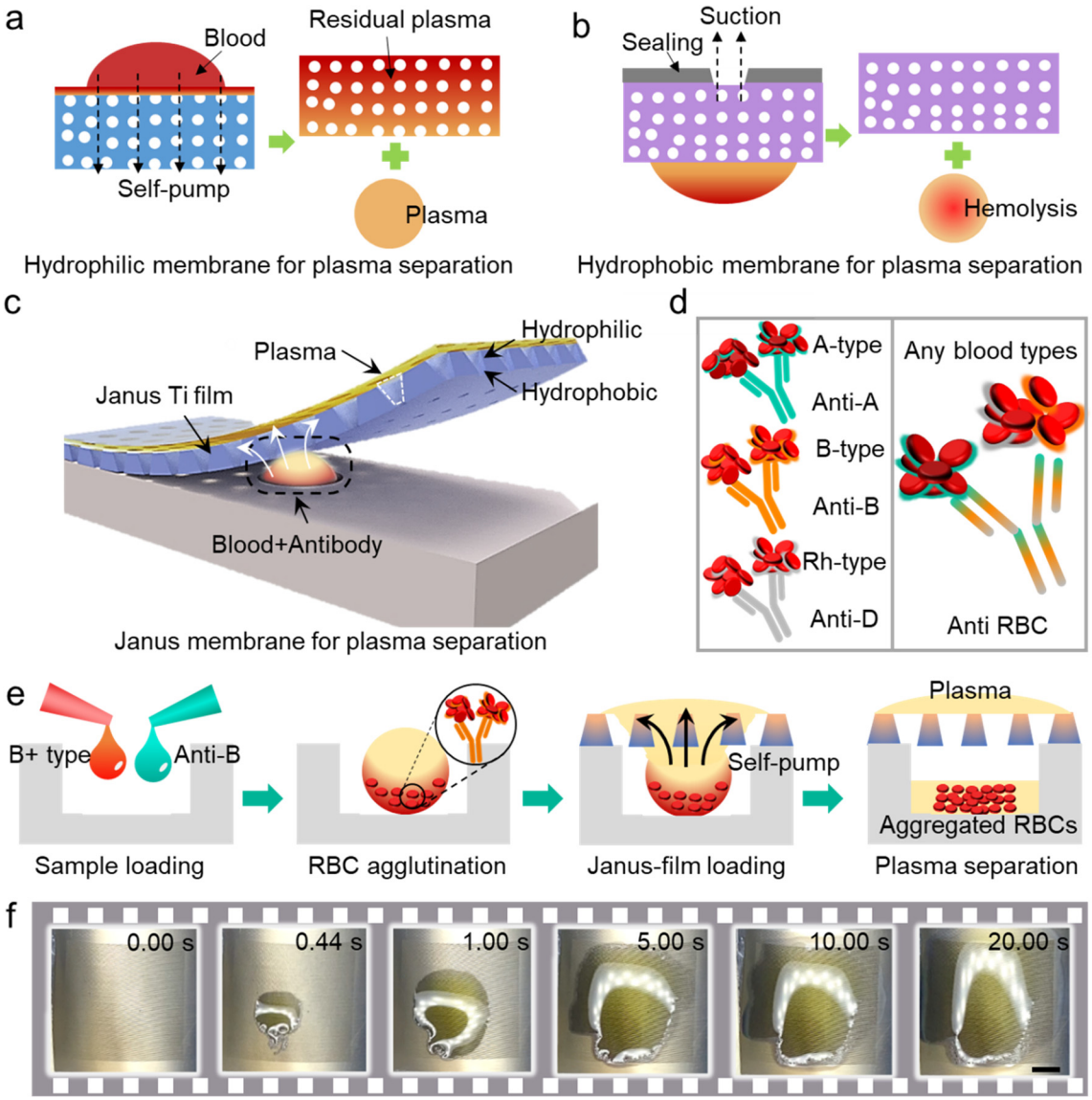

Fig. 1 The high-performance plasma separation method. a) Illustration of the hydrophilic membrane for plasma separation. It can provide a self-driving capillary force to let the plasma flow. But the hydrophilic membrane inevitably absorbed several plasma, decreasing the plasma yield. b) Schematic illustration of plasma extraction through a hydrophobic membrane which can effectively improve the residual plasma. The superhydrophobicity property of the membrane hinders the generation of capillary force and may induce hemolysis. c) Schematic diagram of the plasma separation process with the help of a Janus membrane. The Janus membrane can not only spontaneously extract the plasma, but also decrease the residual plasma. d) RBC agglutination reaction. Anti-A, anti-B and anti-D can induce RBC agglutination reactions of blood type A, B and RhD+, respectively. The anti-RBC antibody can induce the RBC agglutination reaction of any blood types. e) Schematic diagram of the plasma separation process with RBC agglutination assistance. f) Video stills of the plasma extraction process of 15 μL whole blood. The plasma separation process can be finished within 20 s. The scale bar: 2 mm.

increase the plasma extraction yield (~70%). However, the superhydrophobicity property of the filter membrane hinders the generation of self-pumped capillary force (Fig. 1b). Moreover, the manual operation for separating plasma with a hand-powered pipette may prevent reproducible results and induce the rupture of red blood cells (Fig. 1b). Besides, the large flow resistance induced by nanopores is still an issue.

Recently, Janus membrane technology has been widely developed which can generate pressure gradients that drive liquid to transport from the hydrophobic side to the hydrophilic side but block the liquid flow in the reverse direction.[14–23] This not only opens a means for continuous liquid directional transportation without any external pump, but also effectively solves the problem of residual liquid.[24] Therefore, there is great potential to employ Janus membranes for ideally separating plasma from whole blood. Here, we report a novel method for POCT plasma separation from whole blood by combining the Janus membrane technology with the red blood cell (RBC) agglutination reaction (Fig. 1c). Specifically, the RBC agglutination reaction can form large RBC aggregates to separate plasma from blood cells. The Janus membrane can be treated as a "pump" to induce liquid flow, where the micropores on the Janus membrane, as a microfilter, can block the RBC aggregates. After continuous RBC aggregate formation, self-pumping of blood flow, and microfiltration, high performance plasma separation is achieved with a plasma yield of ~80% and plasma purity of ~99.99%. More importantly, the membrane retains the same performance (plasma yield: ~80%, plasma purity: 99.99%) at a high hematocrit level (*e.g.*, 85%). Attributed to the continuous liquid flow and large micropores, the plasma separation is extremely fast (~80 s).

2. Results

Plasma separation based on a Janus membrane and RBC agglutination reaction

Titanium foil was chosen to construct the Janus membrane due to its good biocompatibility.[25] Fig. 1c shows the schematic of the high-performance plasma separation method. The Janus titanium membrane can continuously transport plasma from its superhydrophobic side to the superhydrophilic side without any external forces. In order to prevent clogging and improve the plasma yield, the RBC agglutination reaction was employed to form large RBC aggregates (Fig. 1d). Direct agglutination of RBCs occurs when the corresponding antibodies match the antigens on the surface of RBCs.[26] For example, RBC agglutination can be created *via* blood type A with anti-A, blood type B with anti-B, blood type AB with anti-A/anti-B, blood type RhD+ with anti-D, and anti red blood cells (anti-RBC) with any blood types, respectively (Fig. 1d, S1 and S2† for more details). 15 μl whole blood (*e.g.*, B Rh+) and 15 μl antibodies were initially added into a superhydrophobic well which can decrease the liquid adhesion and improve the plasma yield, as shown in Fig. 1e. The RBC agglutination reaction was completed within 1 min, which could be distinguished by our naked eyes (Fig. 1e and S3†). Then, the Janus titanium membrane was loaded with its superhydrophobic surface being in contact with the blood sample. Because of its directional liquid transport property, plasma began to penetrate from the bottom to the top of the membrane. Finally, plasma was successfully separated from whole blood, leaving cell aggregates inside the well (Fig. 1e and S3†). The present method is extremely fast, which can complete plasma extraction within 20 s (Fig. 1f). It was clearly observed that plasma was continuously extracted with no obvious RBCs (Video S1†). This method allowed a typical plasma yield of ~80% and plasma purity of ~99.99%, in which the yield and purity were both higher than those extracted through a hydrophilic titanium membrane with RBC agglutination (plasma yield: ~33.94%, plasma purity: ~97.39%, Fig. S4†). In addition, we developed a clamshell-style plasma separation device based on the Janus film technology and RBC agglutination reaction for better POCT applications (Fig. S5 and S6†). The device was fabricated by 3D printing. The bottom substrate (a2) contained a superhydrophobic (SHP) well which was designed to introduce the whole blood/antibody. And the top cover (a1) had a rectangle pore which could be used to load the Janus titanium film. After plasma separation, the separated plasma on the top surface can be extracted using a pipette. Overall, the present approach is highly effective in rapid POCT plasma separation.

Fabrication of the Janus titanium membrane

The Janus titanium membrane was fabricated by laser micro-drilling, hydrophobicity coating, and selective hydrophilization (Fig. S7†). Firstly, the titanium foil was treated by laser micro-drilling to form a microhole array. Both sides of the fabricated foil were superhydrophilic (TS contact angle: ~2°, BS contact angle: ~6°). The microhole array with a variety of sizes can be flexibly fabricated by simply adjusting the laser power (Fig. S8†). Then, the multipore membrane was modified with hydrophobic SiO_2 particles (Glaco spraying), which was verified by scanning electron microscopy (SEM) images (Fig. S9†). After modification, the membrane became superhydrophobic on both sides (TS contact angle: ~160°, BS contact angle: ~154°). Finally, laser ablation was employed to selectively remove a thin layer of the top surface. As a result, the silica nanoparticles were completely removed (Fig. S9†), which transformed the top surface from being superhydrophobic to superhydrophilic (contact angle: from ~160° to ~2°), while the bottom surface remained superhydrophobic (contact angle: ~153°, Fig. S10†). At present, a femtosecond laser is relatively expensive which is a potential limitation in mass-production of Janus titanium membranes. Luckily, the process of a Janus film can be simplified into two steps: one-side hydrophobic Glaco treatment and microdrilling process. The latter drilling can be achieved through a mechanical mini-drill (Fig. S11†). Thus, the fabrication method can be expanded to mass-production through Glaco spraying

treatment and commercial microdrilling. We further tested the wetting properties of plasma and blood on the fabricated Janus surface (Fig. S12†). The plasma/blood contact angles (PCA/BCA) were ~8°/19° and ~150°/152° on the superhydrophilic and superhydrophobic surface, respectively. The chemical composition change after each step was also investigated by using an energy dispersive X-ray spectrometer (EDS). Compared with the Glaco-treated surface, the atomic content of the silicon element in the laser-treated surface decreased from 5.60% to 0.45% (Fig. S13†), indicating the successful removal of the SiO_2 nanoparticles on the Janus titanium membrane.

Unidirectional liquid transport properties

The liquid transport capacity on the Janus membrane was investigated by continuously dropping plasma onto its both sides. Once the plasma droplet came into contact with its superhydrophobic side, it was rapidly self-pumped through the superhydrophobic surface and wetted superhydrophilic side (Fig. 2a, Video S2†). A continuous supply of plasma droplets produced an increasingly large liquid film on the superhydrophilic surface, while the superhydrophobic surface still kept unwetted and no residual liquid remained on the superhydrophobic surface. In contrast, when a plasma droplet came into contact with the superhydrophilic surface, it rapidly spread and was blocked to penetrate into the hydrophobic side (Fig. 2b, Video S3†). These results suggested that the Janus membrane was able to unidirectionally transport plasma and minimize the residual plasma. Here, the Janus titanium membrane was loaded on the top of a blood droplet. As a result, it can directly come into contact with the supernatant of the mixed sample and achieve transport of plasma to its superhydrophilic surface, which was beneficial to obtaining a high plasma yield/purity. The liquid transport properties were further investigated by continuously introducing water or plasma droplets to the bottom surface (Fig. 2c). Fig. 2d and e show the actual transport progress of the water/plasma droplet, respectively. Once a water/plasma droplet came into contact with the bottom surface, it quickly passed through the Janus membrane. With the continuous supply of water/plasma droplets, water/plasma would enrich the pipe and keep self-ascending until a balance was achieved. The maximum self-ascending height of water/plasma was 8 mm/4.5 mm which determined the maximum plasma extraction volume (Fig. 2f). For example, once using a 5 × 5 mm^2 Janus membrane to separate the plasma, the maximum volume of plasma extraction was about 112.5 μL (4.5 mm × 5 mm× 5 mm). In fact, for separating a 30 μL mixed sample (15 μL whole blood (hematocrit: ~50%) + 15 μL antibody), its liquid component (~22.5 μL) was far less than the maximum volume (112.5 μL). Therefore, the Janus membrane is competent to achieve spontaneous plasma transport and prevent the plasma from transporting back.

Plasma separation performance

The plasma yield and purity are two key metrics that directly represent the performance of a blood plasma separation technology. In our experiments, purity is defined as the ratio

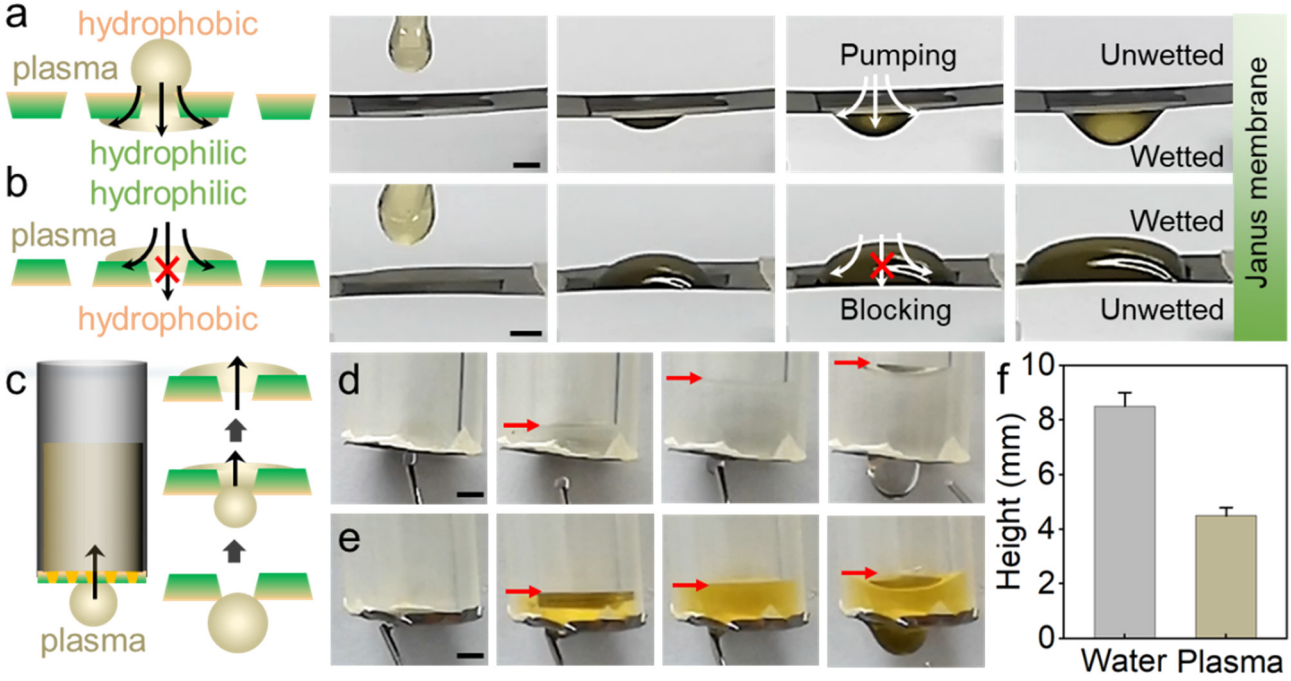

Fig. 2 Demonstration of unidirectional liquid transport properties. a) and b) Flow behaviors of plasma on a Janus membrane. c) Spontaneous plasma transport on a Janus membrane. d) and e) Actual transport process of water and plasma. f) Self-ascending height of water and plasma. All scare bars: 2 mm.

of the number of RBCs in extracted plasma from the hydrophilic surface to that of original RBCs in whole blood. And, the plasma yield is the ratio of the plasma volume on the superhydrophilic surface to the theoretically available plasma volume. The detailed descriptions of the yield and purity can be found in the Experimental section. Firstly, we investigated the plasma separation of various whole blood volumes (~45% hematocrit, 10–100 μL) and analyzed how the sample volume affected the separation results (Fig. 3a and b). Briefly, the plasma yield was ~80% for 10–20 μL whole blood, which was higher than that of traditional plasma separation membranes (Fig. 3a, Table 1).[4,8,9,26–29] Once the blood volume increased, the plasma yield decreased. For example, once we introduced 100 μL whole blood into the well, the plasma yield dropped to ~59.3%. Meanwhile, we found no significant decrease of the plasma purity once the whole blood volume increased from 10 μL to 100 μL (Fig. 3b). All the plasma purity was ~99.99% after separation. Excitingly, our work provides a promising way to obtain good results in both yield (~80%) and purity (~99.99%) (Table 1). In addition, we also tested the influence of the microhole size on the separation results in terms of yield and purity. Once the size of the microhole increased (from 23 μm to 38/41 μm), there was no significant drop in the plasma yield and purity (Fig. 3c). As a result, the yield and purity were both high enough (yield: ~79.2% for the 23 μm hole, ~83.3% for the 38 μm hole and ~85.4% for the 41 μm hole, each purity: ~99.99%) (Fig. 3c). The dimensions of the Janus membrane were further investigated to obtain better plasma separation performance. The results suggested that the yield can reach 85.4% and the purity was 99.99% when using a large film (12 × 12 mm^2). Once we selected a small size Janus film, there was no significant drop in the plasma yield and purity (yield: 84.4% for the 10.5 × 10.5 mm^2 membrane, 78.1% for the 9 × 9 mm^2 membrane, 83.3% for the 7.5 × 7.5 mm^2 membrane, 84.4% for the 6 × 6 mm^2 membrane and 84.4% for the 4.5 × 4.5 mm^2 membrane, each purity: ~99.99%). Moreover, we investigated plasma separation in different blood types with the aid of antibodies (anti-A, anti-B, anti-D and anti-RBC). The obtained yield and purity were both ultra-high (yield: 84.7%, purity: 99.99%, Fig. 3f) once we utilized the anti-A antibody. We found no significant drop in the plasma separation performance once we used anti-B and anti-D antibodies (yield: 82.1% for the anti-B antibody and 84.4% for the anti-D antibody, each purity: 99.99%, Fig. 3f). When we used the anti-RBC antibody, the plasma separation yield was 78.69% through using the present separation method, in which the plasma yield was significantly lower than that using the anti-A antibody (84.7%). In fact, the plasma yield through using the anti-RBC antibody was still much higher than that of most traditional plasma separation membranes (Table 1).[4,8,9,26–29]

The hematocrit level, the volume percentage of RBCs in blood, directly impacts the performance of plasma separation

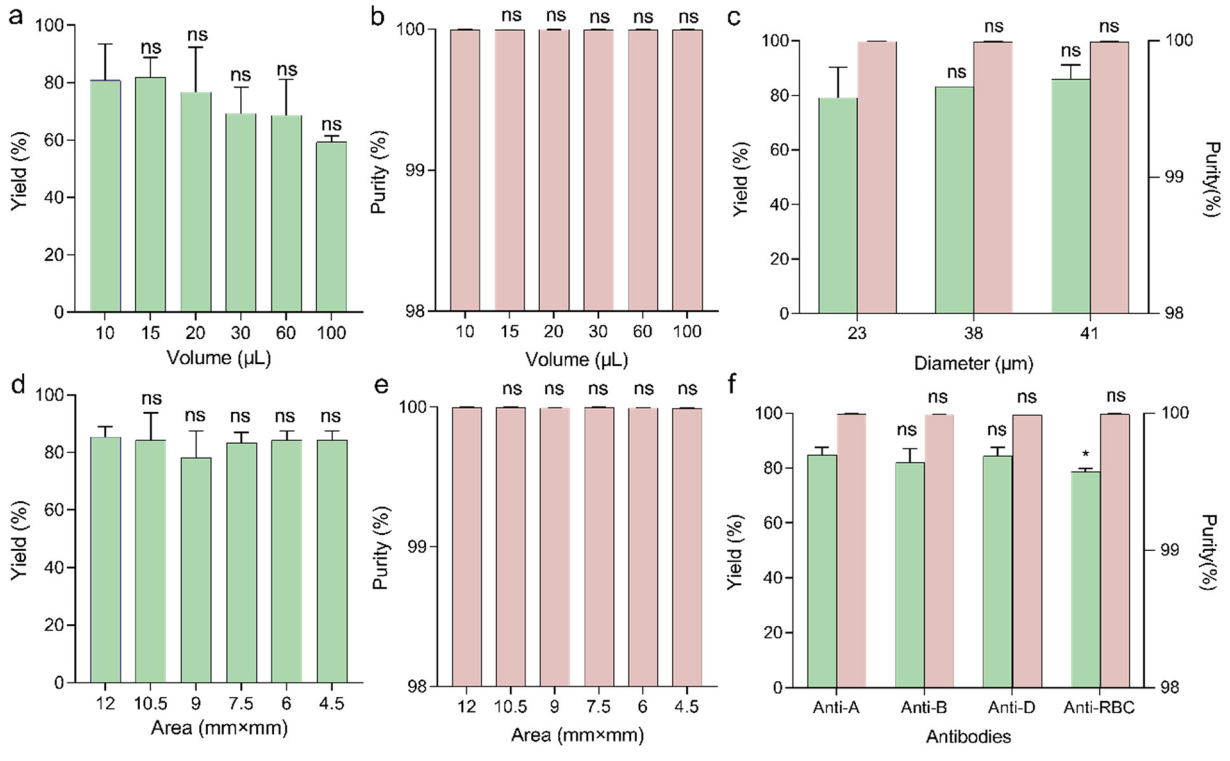

Fig. 3 Yield/purity investigations. a and b) Plasma yield/purity obtained from different blood volumes. c) The relationship between the plasma yield/purity and different pore sizes. d and e) Plasma yield/purity obtained by different membrane dimensions. f) The dependence of the plasma yield/purity on different antibodies (anti-A, anti-B, anti-D and anti-RBC). Results in all histograms were plotted as the mean ± s.d. (n = 3), *p < 0.05 and ns means not significant.

Table 1 Comparison between our results of plasma separation performance and those of state-of-the-art plasma filter membranes. N.P. means not provided in the literature

Ref.	Yield (%)	Purity (%)	Hematocrit range (%)	Separation time (s)	Membrane wetting property
Liu *et al.*[4]	~70	N.P.	N.P.	~600	Superhydrophobic
Hauser *et al.*[5]	~65	N.P.	35–55	~600	Hydrophilic
Lu *et al.*[11]	60	99	30–60	1200	Hydrophilic
Guo *et al.*[6]	~11	N.P.	45	316	Hydrophilic
Liu *et al.*[12]	<30	N.P.	N.P.	420	Hydrophilic
Shim and Ahn[13]	~12	N.P.	43	~120	Hydrophilic
This work	**~80**	**99.99**	**15–85**	**~80**	**Janus**

devices. Conventional membrane separation technologies showed severe drops in the plasma purity or yield with high hematocrit levels.[1] Here, to further demonstrate the plasma separation capacity of the proposed method, we separated plasma in artificially spiked blood samples that had hematocrit levels of 15–85%. The results were shown in Fig. 4, which demonstrated a distinct plasma extraction performance from the conventional separation methods. Specifically, for a hematocrit level of 15% the plasma yield was ~84.7% and the purity of the separated plasma was ~99.99%. Once the hematocrit level (35–85%) of the whole blood increased, there was no significant drop in the plasma yield. And, the separation yields were all larger than 80%. Although the plasma purity in the hematocrit level of 60% (99.98%) was significantly lower than that of 15% (99.99%), it was high enough for most of the plasma-based applications.

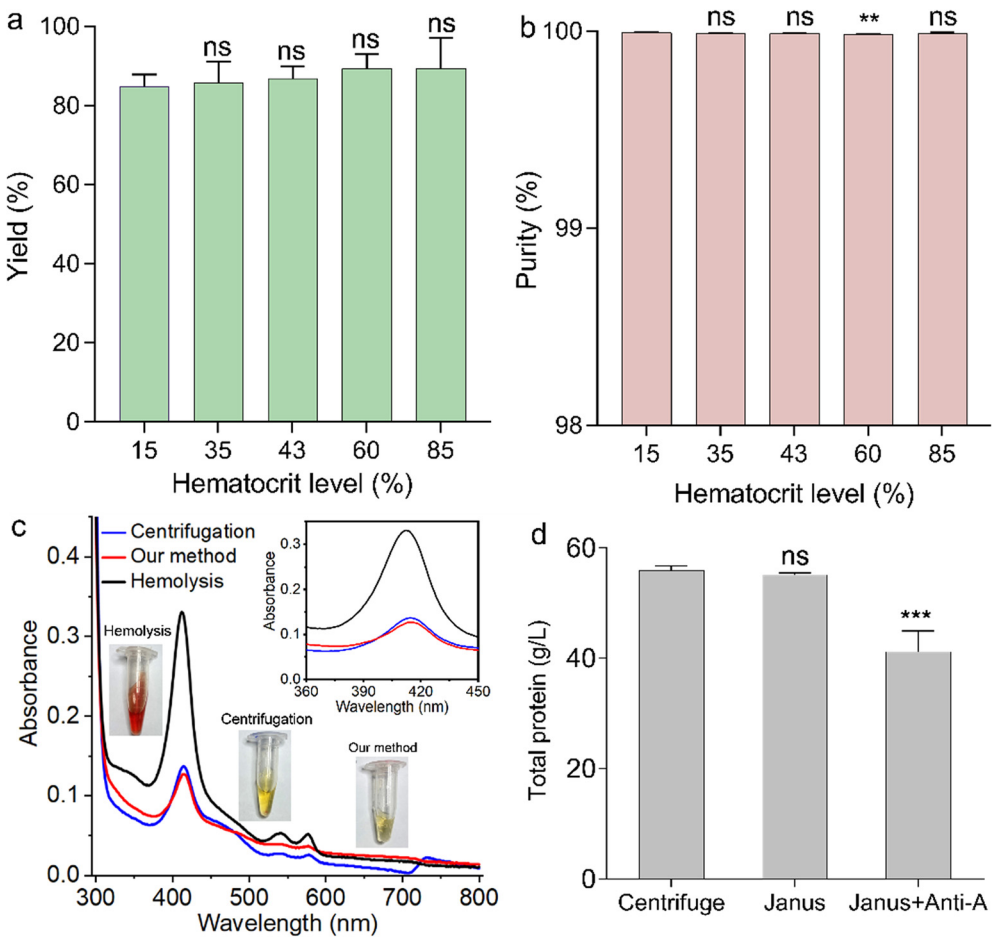

Fig. 4 Hematocrit level, hemolysis and protein loss studies. a and b) Plasma yield/purity obtained from whole blood samples with different hematocrit levels. c) Absorption spectrum of hemolytic blood, plasma *via* centrifugation and plasma separated *via* our method. The inset images show the actual images of the hemolytic plasma, centrifuged plasma and plasma extracted through our method. The hemolytic plasma was red, and the latter two plasma were both yellow, indicating that there was no obvious hemolysis through using our method. d) Protein recovery of the centrifugation method, Janus film with pre-sediment and our method. Results in all histograms were plotted as the mean ± s.d. (n = 3), $^{**}p < 0.01$, $^{***}p < 0.001$, and ns means not significant.

The purities of other cases were all ~99.99% (Table 1, Fig. 4a and b). The above results indicated the feasibility of the proposed plasma extraction technique to separate plasma from whole blood with almost all the hematocrit levels.

In addition, hemolysis should be avoided in a plasma separation device since hemolysis will release hemoglobin in plasma and hinder subsequent analysis.[1] So people usually test the hemoglobin concentration to determine whether hemolysis happens. Hemolysis assessment is carried out by measuring the absorbance of plasma samples at 300–800 nm using a UV-vis spectroscopy. Usually, there is a maximal absorbance peak at 414 nm. It is widely accepted that absorbance values at 414 nm (the abs.-max of hemoglobin) of 0.3 units at this wavelength are indicative of plasma that is non-hemolyzed.[30,31] Centrifugation is the gold standard for plasma separation. Thus, we compared the absorbance values of the extracted plasma through our method with those of centrifuged plasma. The results demonstrated that our method could obtain a similar hemoglobin concentration (red line in Fig. 4c) to that obtained through centrifugation (blue line in Fig. 4c). Actual separated plasma with no obvious red color further indicated prevention of hemolysis *via* our method (Fig. 4c inset).

Another metric used to evaluate plasma separation performance is the loss of the protein. Here, the total protein concentration was 55.96 g L^{-1} *via* centrifugation. Once we used the present plasma separation method (Janus membrane + RBC agglutination), the total protein concentration was 41.2 g L^{-1} which was significantly lower than that *via* centrifugation (55.96 g L^{-1}, Fig. 4d). We thought that introducing antibodies would dilute the total protein concentration inevitably, while it did not mean loss of the target protein. To explore if the protein was lost in the separation process, we utilized a Janus membrane to separate the plasma from whole blood which was allowed to settle in 30 min. We found that there was no significant drop in the total protein concentration. And the total protein concentration was 55.2 g L^{-1} which was similar to that of centrifugation (55.96 g L^{-1}). The results indicated that our plasma separation method had minimal loss of the target protein. Overall, the method can extract plasma from a small volume of blood with high performance.

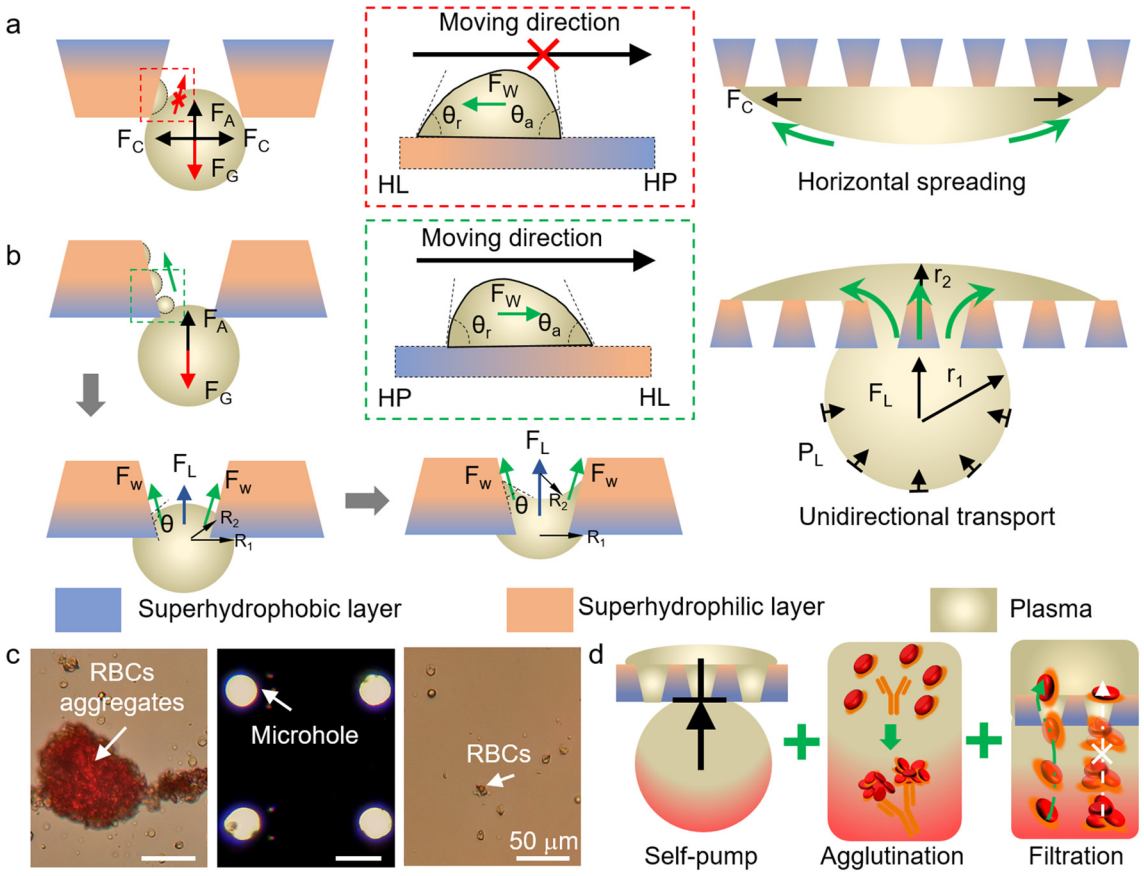

Fig. 5 Mechanism investigations of the plasma separation method. a) Wetting/transport process analysis of a plasma droplet on the hydrophilic surface. b) Driving force analysis in the wetting/transport process of a liquid droplet on the hydrophobic surface. c) Images of RBC aggregates, filtering microholes and single RBCs. d) Schematic illustration of the plasma separation mechanism. F_A, F_G, F_C, F_W and F_L are short for the adhesion force, gravity, capillary force, wetting gradient force and Laplace force, respectively. HP and HL represent hydrophobic and hydrophilic, respectively.

Plasma separation mechanism

To understand the unidirectional liquid transport, we firstly investigated the inner morphology of the micropores (Fig. S14†). The SEM images showed that there were numerous nanostructures inside the tapered micropores, where the nanostructures on the lower side were bigger than those on the upper side. Then, the driving force for plasma separation was deeply investigated (Fig. 5). Usually, the plasma separation consisted of wetting and transport processes, in which the former determined whether the latter would take place. If the water/plasma droplet came into contact with the bottom superhydrophilic surface of the Janus membrane (Fig. 5a), the droplet was subjected to three forces: gravity (F_G), adhesion force (F_A), and capillary force (F_C).[32] The droplet adhered steadily to the lower surface due to the force balance in the vertical direction (Fig. 5a). The wetting process can be analyzed as follows. The wetting gradient from the hydrophilic side to the hydrophobic side led to an asymmetric liquid contact angle, thus creating a wetting gradient force F_w.[33] The wetting gradient force can be quantified as $F_W = 2\pi r\gamma\ (\cos\theta_a - \cos\theta_r)$, where γ, r, θ_a, and θ_r are the surface tension of the liquid, the radii of the micropore, the advancing angle and the receding angle, respectively. Here, the advancing angle was larger than the receding angle (Fig. 5a median), resulting in a resistance force. Thus, the droplet cannot wet the whole microhole. As a result, the liquid spread horizontally because of the existence of capillary force (Fig. 5a). Once the droplet came into contact with the lower superhydrophobic surface, the wetting gradient force functioned as a driving force to wet the interior of the microholes (Fig. 5b) because the wetting gradient of the microholes can create a small advancing angle and a large receding angle. During the wetting process, another Laplace force was created due to the asymmetric droplet meniscus (Fig. 5b). The Laplace force[34–36] can be expressed as $F_L = \gamma\cdot(1/R_1 + 1/R_2)\cdot S$, where R_1/R_2 is the radius of curvature of the lower/upper droplet and S is the contact area. R_1 remained the same during the wetting process, while R_2 was initially negative in the hydrophobic part of the micropore and changed to positive in its hydrophilic region. As a result, the driving force ($F_L + F_W$) increased gradually during the wetting process. After completing the wetting process, the droplet reached the superdydrophilic surface of the Janus membrane and the asymmetry meniscus of the droplet emerged (Fig. 5b). Specifically, the lower liquid remained spherical, and the upper droplet spread to form a thin liquid membrane. At this point, the liquid transport process started. And another Laplace force ($F_{L1} = \gamma\cdot(1/r_1 - 1/r_2)\cdot S1$, Fig. 5) emerged to continuously self-pump the liquid until a self-ascending balance was achieved. In addition, the Laplace force for plasma transport was smaller than that for water due to the smaller surface tension of plasma (plasma/water: 0.057/0.072 N m^{-1}).[37] The smaller driving force balanced to the gravity of a less ascending liquid, which explained why the ascending height of plasma was smaller than that of water (Fig. 2f). Next, the microfiltration process was analyzed to better understand the separation method. In our study, most of the RBCs were transformed into aggregates that had a size range of 10 μm to >100 μm (Fig. 5c and S15†). The larger one (size >100 μm) consisted of hundreds of RBCs and occupied most of the volume of RBCs (Fig. S16†). The large aggregates can be easily blocked by the micropores on the Janus film (Fig. 5c), resulting in creation of high plasma purity. Combining the unidirectional liquid transport capacity with microfiltration (Fig. 5d), high-performance plasma separation is successfully achieved.

3. Discussions

For simplicity, we used anti-A/B/D antibodies to induce RBC agglutination in whole blood. To improve the robustness of this method, the anti red blood cell (anti-RBC) antibody[38] was chosen which can induce RBC agglutination of any blood types. The anti-RBC antibody can effectively replace anti-A/B/D and induce the RBC agglutination reaction of any blood types (Fig. S2†). We also tested the RBC agglutination rate with varying levels of the aggregation agent (Fig. S17†). Plasma separation using the anti-RBC antibody can also obtain a high yield (~78.69%) and a high purity (~99.99%) (Fig. 3f and S18†). In addition, we compared the dependence of introducing anti-RBC or no anti-RBC on the plasma separation yield and purity (Fig. S19†). The plasma yield through a Janus membrane without the addition of anti-RBC was about 7.3% which was significantly lower than that with anti-RBC (78.69%). In contrast, the plasma purity significantly decreased to 29.57% once there was no addition of anti-RBC inside the whole blood. The experiments proved that the use of the anti-RBC antibody can effectively improve the plasma separation performance and extend the applicability of our separation approaches to all blood samples.

Moreover, we further explored whether adding antibodies to the blood will influence the diagnosis results. Yang *et al.*[39] and the Erickson group[38] demonstrated that the plasma separated *via* the RBC agglutination reaction had the same concentrations of glucose and ferritin as those obtained *via* conventional methods, respectively. Here, we further investigated this issue through checking whether adding antibodies to the blood will influence the blood glucose concentration. Blood with a hematocrit level of 50% was chosen and a blood glucose meter was used to measure the blood glucose level. The results (Fig. S20 and S21†) showed that the glucose concentrations of whole blood, blood after centrifugation, and blood after RBC agglutination were 5.1, 11.4 and 3.9 mmol L^{-1}, respectively. The volume ratio between whole blood and anti-D was 1 : 1 and the volume ratio of plasma/blood cells was 0.5 : 0.5 (hematocrit level: 50%), which indicated that the plasma had 3 times dilution. Also, the anti-D reagent didn't contain any glucose. Therefore, the actual glucose level through RBC agglutination was 11.89 mmol L^{-1}, which was similar to the actual value

(11.4 mmol L^{-1}). Thus, adding antibodies to the blood would not influence the diagnosis of the glucose level.

4. Conclusion

In conclusion, we proposed a blood plasma separation technique aimed at overcoming the present issues in plasma extraction through filtration membranes. The RBC agglutination reaction can effectively form large RBC aggregates and separate plasma from them. The Janus membrane can spontaneously transport plasma from its hydrophobic side to the hydrophilic side. The micropores located on the membrane can block the RBC aggregates and help to obtain ultrapure plasma. Within 80 s, we can achieve an ~80% plasma yield and ~99.99% plasma purity from a small volume of whole blood (15–85% hematocrit). Meanwhile, our method can obtain a similar hemoglobin concentration to that of centrifugation, demonstrating that no obvious hemolysis happens. We envision that the high-performance plasma separation method will open up opportunities for POCT applications in remote areas and allow robust detection of low-concentration analytes from whole blood.

5. Experimental section

Preparation of the Janus titanium membrane

Titanium foil (thickness: 30 μm, New Metal Material Tech. Co., Ltd, Beijing) with uniform microhole arrays was drilled by using a regenerative amplified Ti:sapphire femtosecond laser system (Legend-Elite-1 K-HE, Coherent, USA) that generates 104 fs pulses at a repetition rate of 1 kHz with a central wavelength of 800 nm. The fabrication process was controlled by using a 2D scanning galvanometer (Scanlab GamH, hurrySCAN II 10, Germany). The diameter of the focus spot was about 20 μm. The interval between adjacent holes was kept at 150 μm. The fabricated titanium foil was superhydrophilic after laser drilling. Then, superhydrophilic aluminum foil was modified to become superhydrophobic by spraying Glaco (Glaco Mirror Coat Zero, Soft 99 Ltd, Japan) 3 times. Finally, the lower surface was scanned by using a laser (50 mW) at a speed of 30 mm s^{-1} and a scanning space of 10 μm.

Preparation of the silicone substrate

A hole with a diameter of 6 mm was firstly punched on a silicone gel (Jiangsu Gefang New materials, Jiangsu, China) with a thickness of 1.5 mm. Then a clean glass slide and the silicone gel were treated with oxygen plasma (Mingheng PDC-MG, 50 s, 75 W, 100 Pa). After bonding with a suitable press, the microchip was treated at 65 °C for 30 min to complete bonding. Finally, Glaco spray was applied to make the surface of the gel and the sidewall of the hole superhydrophobic (Fig. S22†).

Preparation of the plasma separation device

The clamshell-style plasma separation device was customized from Yichang Youchuang 3D Intelligent Technology Co., Ltd (China). For mass-production, the company charges the 3D printing device through weight, and 1 g usually costs 0.5 ¥. Our plasma device weighed ~4 g. Therefore, the whole price was ~2 ¥.

Blood samples

The blood samples and their hematocrit levels were provided by the First Affiliated Hospital of University of Science and Technology of China. All experiments were conducted according to hospital guidelines ("Human Research Ethics Guide") and approved by the Institutional Ethical Committee (IEC) of the hospital (2021-RE-012). All blood samples were stabilized with anticoagulant additives, stored in vacutainer test tubes containing heparin, citrate, and EDTA at 4 °C, and used within 7 days of collection. Blood samples with abnormal hematocrits were prepared with type A+ human red blood cells. The blood cells were spun down and concentrated in a centrifuge, and were resuspended to plasma to form a variety of hematocrit values.

Plasma separation

Anti-A/B/D (Beijing Solarbio Science & Technology Co., Ltd, Beijing, China) was initially introduced to the well. The anti red blood cell antibody was purchased from Rockland Antibodies, USA. Then, the same volume of whole blood as the corresponding antigen was added to the antibody droplet. After 1 min waiting for reaction completion, a Janus membrane was loaded and brought into contact with the top of the mixed droplet. About 20 s later, the self-pumping process was completed. Through sucking the plasma from the membrane surface, pure plasma can be collected for the following analysis. For plasma separation by centrifugation, the whole blood was centrifuged for 10 min at 2000*g* in an AccuSpin™ Micro 17 centrifuge (Thermo Fisher Scientific, Rockford, IL), and the plasma was recovered using a pipette and stored for analysis.

Unidirectional liquid flow tests

Water/plasma droplets of ~20 μl per droplet were dripped onto either superhydrophobic or superhydrophilic sides of the Janus titanium membrane. For testing the liquid transport properties, the Janus membrane was initially attached to the bottom of a tubular container, and then continuous water/plasma obtained by centrifugation was introduced using a needle to the bottom side of the Janus titanium membrane. In the end, a ruler was employed to test the final self-ascending height.

Characterization

The surface topographies of the treated titanium samples were characterized by using secondary electron SEM (ZEISS

EVO18). Field-emission transmission electron microscopy energy dispersive X-ray analysis (JEM 2100F, JEOL, Japan) was used to characterize the different element components of the titanium samples. A CA100C contact-angle system (Innuo, China) was used to measure the water CAs (4 μL water). The optical images were taken using a charge-coupled device camera.

Plasma performance analysis

Here, the extraction yield is defined as the plasma volume on the superhydrophilic surface of the Janus membrane over the theoretically available plasma volume. In our experiments, the injected antibody had the same volume as the whole blood. And the liquid situated on the hydrophilic surface contained plasma and residual antibodies (V_{Plasma} : $V_{Antibody}$ = 1 − hematocrit : 1). Thus, the plasma yield can be expressed as: Yield = $V_{SHL}/V_B(2 - hct\%)$, where V_{SHL} is the liquid volume on the superhydrophilic surface of the Janus membrane, V_B is the injected antibody volume and hct% is the hematocrit level. We firstly measured the increasing quality of the Janus membrane to calculate the V_{SHL}. Then, the yield can be calculated through the above equation.

Purity is defined as the ratio of the number of RBCs in the extracted plasma from the hydrophilic surface to that of original RBCs in whole blood, Purity = $1 - C_H/C_O$. Here, C_H is the number of RBCs in the extracted plasma (from the hydrophilic surface) and C_O is the number of RBCs in the whole blood. We used the hemocytometer counting method with a Bright-Line hemocytometer (Hefei Ruijie Biotechnology Co. LTD, Anhui, China) to measure the number of the original blood cells (C_O) and the RBCs in the extracted plasma (C_H). Then, the purity can be calculated through the above equation.

Hemolysis assessment was carried out by measuring the absorbance of 3 μL samples at 300–800 nm using UV-vis spectroscopy (Solid3700, Shimadzu Corporation). The protein recovery was assessed using an Abbkine BCA Protein Quantification Kit (Kit 3001, Abbkine, China). The assay was performed according to the instructions by the supplier. The samples were pipetted in duplicate into a 96-well plate (734–2327, VWR, Spånga, Sweden), and absorbance measurements were carried out at 562 nm on a plate reader (Thermo, America).

Statistical analysis

All results were presented as the mean ± standard deviation. The error bars correspond to the standard deviation of three independent experiments. One-way ANOVA was performed using GraphPad Prism 7.0, and the statistical significance is defined as follows: $*p < 0.05$, $**p < 0.01$, $***p < 0.001$, and $****p < 0.001$; NS means not significant.

Conflicts of interest

The authors declare no conflict of interest.

Acknowledgements

This work was supported by the National Natural Science Foundation of China (No. 52105583), the Primary Research and Development Plan of Jiangsu Province (BK20221386), the Innovation and Entrepreneurship Training Program for College Students (202210332047Z), the Fundamental Research Funds for the Central Universities (WK911000057), the Project of the Science and Technology Innovation of Anhui province (2017070802D146; 2018080402A009), and the Key Programs for Research and Development of Anhui Province (No.1704a0802153). The USTC Center for Micro and Nanoscale Research and Fabrication is acknowledged.

References

1 M. Kersaudy-Kerhoas and E. Sollier, *Lab Chip*, 2013, **13**, 3323–334617.
2 W. S. Mielczarek, E. A. Obaje, T. T. Bachmann and M. Kersaudy-Kerhoas, *Lab Chip*, 2016, **16**, 3441–3448.
3 A. Lenshof, A. Ahmad-Tajudin, K. Järås, A. Swärd-Nilsson, L. Åberg, G. Marko-Varga, J. Malm, H. Lilja and T. Laurell, *Anal. Chem.*, 2009, **81**(15), 6030–6037.
4 C. Liu, S. Liao, J. Song, M. G. Mauk, X. Li, G. Wu, D. Ge, R. M. Greenberg, S. Yang and H. H. Baua, *Lab Chip*, 2016, **16**, 553–560.
5 J. Hauser, G. Lenk, J. Hansson, O. Beck, G. Stemme and N. Roxhed, *Anal. Chem.*, 2018, **90**(22), 13393–13399.
6 Z. Lu, E. Rey, S. Vemulapati, B. Srinivasan, S. Mehta and D. Erickson, *Lab Chip*, 2018, **18**, 3865–3871.
7 J. Hauser, G. Lenk, S. Ullah, O. Beck, G. Stemme and N. Roxhed, *Anal. Chem.*, 2019, **91**(11), 7125–7130.
8 D. W. Inglis, K. J. Morton, J. A. Davis, T. J. Zieziulewicz, D. A. Lawrence, R. H. Austind and J. C. Sturm, *Lab Chip*, 2008, **8**, 925–931.
9 B. Kim, S. Oh, D. You and S. Choi, *Anal. Chem.*, 2017, **89**, 1439–1444.
10 M. Faivre, M. Abkarian, K. Bickraj and H. A. Stone, *Biorheology*, 2006, **43**, 147–159.
11 T. A. Shatova, S. Lathwal, M. R. Engle, H. D. Sikes and K. F. Jensen, *Anal. Chem.*, 2016, **88**, 7627–7632.
12 K. R. Baillargeon, L. P. Murray, R. N. Deraney and C. R. Mace, *Anal. Chem.*, 2020, **92**, 16245–16252.
13 W. J. Guo, J. Hansson and W. V. D. Wijngaart, *Anal. Chem.*, 2020, **92**, 6194–6199.
14 D. Miao, Z. Huang, X. Wang, J. Yu and B. Ding, *Small*, 2018, **14**, 1801527.
15 Y. Wang, X. Liang, H. Zhu, J. H. Xin, Q. Zhang and S. Zhu, *Adv. Funct. Mater.*, 2020, **30**, 1907851.
16 H. X. Wang, J. Ding, L. M. Dai, X. G. Wang and T. Lin, *J. Mater. Chem.*, 2010, **20**, 7938–7940.
17 H. Hou and Z. G. Guo, *J. Mater. Chem. A*, 2019, **7**, 12921–12950.
18 Q. Zhang, Y. Li, Y. Yan, X. Zhang, D. Tian and L. Jiang, *ACS Nano*, 2020, **14**, 7287.

19 B. Dai, K. Li, L. Shi, X. Wan, X. Liu, F. Zhang, L. Jiang and S. Wang, *Adv. Mater.*, 2019, **31**, 1904113.
20 L. X. Shi, X. Liu, W. S. Wang, L. Jiang and S. T. Wang, *Adv. Mater.*, 2019, **31**, 1804187.
21 F. Ren, G. Li, Z. Zhang, X. Zhang, H. Fan, C. Zhou, Y. Wang, Y. Zhang, C. Wang, K. Mu, Y. Su and D. Wu, *J. Mater. Chem. A*, 2017, **5**, 18403–18408.
22 Z. Zhang, Y. Zhang, H. Fan, Y. Wang, C. Zhou, F. Ren, S. Wu, G. Li, Y. Hu, J. Li, D. Wu and J. Chu, *Nanoscale*, 2017, **9**, 15796–15803.
23 Y. Yang, X. Yang, L. Fu, M. Zou, A. Cao, Y. Du, Q. Yuan and C. H. Yan, *ACS Energy Lett.*, 2018, **3**, 1165–1171.
24 L. L. Yan, X. B. Yang, Y. Q. Zhang, Y. D. Wu, Z. J. Cheng, S. B. Darling and L. Shao, *Mater. Today*, 2021, **51**, 626–647.
25 Y. Meng, X. Li, Z. Li, C. Liu, J. Zhao, J. Wang, Y. Liu, X. Yuan, Z. Cui and X. Yang, *ACS Appl. Mater. Interfaces*, 2016, **8**(9), 5783–5793.
26 M. Li, J. Tian, M. A. Tamimi and W. Shen, *Angew. Chem.*, 2012, **124**, 5593–5597.
27 Z. D. Lu, E. Rey, S. Vemulapati, B. Srinivasan, S. Mehta and D. Erickson, *Lab Chip*, 2018, **18**, 3865–3871.
28 C. C. Liu, M. Mauk, R. Gross, F. D. Bushman, P. H. Edelstein, R. G. Collman and H. H. Bau, *Anal. Chem.*, 2013, **85**, 10463–10470.
29 J. S. Shim and C. H. Ahn, *Lab Chip*, 2012, **12**, 863–866.
30 C. Dixon, J. Lamanna and A. R. Wheeler, *Lab Chip*, 2020, **20**, 1845–1855.
31 P. Dunne, T. Adachi, A. A. Dev, A. Sorrenti, L. Giacchetti, A. Bonnin, C. Bourdon, P. H. Mangin, J. M. D. Coey, B. Doudin and T. M. Hermans, *Nature*, 2020, **581**, 58–62.
32 S. Yang, K. Yin, D. K. Chu, J. He and J. A. Duan, *Appl. Phys. Lett.*, 2018, **113**, 203701.
33 C. Chen, Z. Huang, L. Shi, Y. Jiao, S. Zhu, J. Li, Y. Hu, J. Chu, D. Wu and L. Jiang, *Adv. Funct. Mater.*, 2019, **29**, 1904766.
34 Y. Hu, W. Qiu, Y. Zhang, Y. Zhang, C. Li, J. Li, S. Wu, W. Zhu, D. Wu and J. Chu, *Appl. Phys. Lett.*, 2019, **114**, 173701.
35 Y. H. Su, S. W. Cai, T. Wu, C. Z. Li, Z. C. Huang, Y. Y. Zhang, H. Wu, K. Hu, C. Chen, J. W. Li, Y. L. Hu, S. W. Zhu and D. Wu, *Adv. Mater. Interfaces*, 2019, **6**, 1901465.
36 J. Jie, B. Hao, Y. Zheng, T. Zhao, R. Fang and J. Lei, *Nat. Commun.*, 2012, **3**, 1247.
37 J. Rosina, E. Kvašňák, D. Šuta, H. Kolářová, J. Málek and L. Krajči, *Physiol. Res.*, 2007, **56**, S93.
38 S. Vemulapati and D. H. Erickson, *Lab Chip*, 2018, **18**, 3285–3292.
39 X. X. Yang, O. Forouzan, T. P. Brown and S. S. Shevkoplyas, *Lab Chip*, 2012, **12**, 274–280.